

International corporations trading Brazilian soy are keystone actors for water stewardship

*Original*

International corporations trading Brazilian soy are keystone actors for water stewardship / De Petrillo, E.; Tuninetti, M.; Ridolfi, L.; Laio, F.. - In: COMMUNICATIONS EARTH & ENVIRONMENT. - ISSN 2662-4435. - 4:1(2023).  
[10.1038/s43247-023-00742-4]

*Availability:*

This version is available at: 11583/2978856 since: 2023-05-27T09:34:52Z

*Publisher:*

Nature Publishing Group

*Published*

DOI:10.1038/s43247-023-00742-4

*Terms of use:*

This article is made available under terms and conditions as specified in the corresponding bibliographic description in the repository

*Publisher copyright*

(Article begins on next page)

## International corporations trading Brazilian soy are keystone actors for water stewardship

Elena De Petrillo <sup>1</sup>, Marta Tuninetti <sup>1</sup>, Luca Ridolfi <sup>1</sup> & Francesco Laio<sup>1</sup>

Transnational corporations play a major, but poorly constrained, role in reallocating global water resources. Here, we couple high-resolution, company-specific trade data with hydrological and crop models to estimate the virtual water trade of the top 9 transnational corporations that trade Brazilian soy. We identify 4429 virtual water flows connecting 1620 Brazilian municipalities with the top-10 soy importing countries and find that the total virtual water flow increased from 43 billion m<sup>3</sup> to 100 billion m<sup>3</sup> between 2004 and 2018. We find that the largest soy traders displace on average twice as much virtual water as top-importing countries, excluding China. For example, in 2018 one transnational corporation exported 15 Gm<sup>3</sup>, almost tripling the Netherlands's virtual water import (the second largest importer at about 5 Gm<sup>3</sup>). Our findings highlight the importance of transnational corporations for achieving water stewardship and sustainable supply chains to support water resource security at municipal and international scales.

<sup>1</sup>Department of Environment, Land and Infrastructure Engineering, Politecnico di Torino, Turin, Italy. ✉email: [elena.depetrillo@polito.it](mailto:elena.depetrillo@polito.it)

Providing a growing population with food, fibre, and fuel is exacerbating the pressure on water ecosystems inducing groundwater depletion<sup>1,2</sup>, river ecosystems impoverishment<sup>3,4</sup>, and alteration of key hydrological processes and variables, such as evapotranspiration and soil moisture<sup>5</sup>. Through international food trade, consumers are increasingly decoupled from the pressure on global water resources (i.e. water footprint, WF<sup>6,7</sup> for the food they consume: up to one-third of it comes from foreign countries<sup>8</sup>). The virtual water trade (VWT) (i.e. water embedded in commodity trade) reconnects the water use occurring in the site of production to the sites of consumption, thus introducing a global dimension to water management. However, to date, two critical aspects prevent the VWT to be an effective tool in supporting decision-making at the government or company's level in achieving their sustainability commitments. The VWT has been studied so far mainly through a country-scale perspective<sup>9–14</sup>, thus disregarding the sub-national environmental heterogeneity that controls the crop unitary water footprint (uWF, m<sup>3</sup>/ton, i.e. the crop water requirement measured during the growing period). Few recent studies have focused on inter-regional VW flows in extended countries such as China<sup>15</sup> and India<sup>16</sup>, while other studies<sup>17,18</sup> stressed the potential of recently released national food trade data that can be adopted to improve the WF assessment.

The second missed aspect is the poor understanding of the role of Transnational Corporations (TNCs) in guiding the increasing pressure of the agricultural sector on water resources. Despite TNCs having been identified as keystone actors of the global production ecosystem<sup>19</sup> and a major driver of the outsized footprint on the biosphere<sup>20</sup>, their possible engagement in the corporate water stewardship has received limited scholarly attention<sup>21</sup>: to date, there remains a poor understanding of the critical role played by Transnational Corporations (TNCs) in driving and managing the water use in the food production system. This knowledge gap limits the extent to which sustainable water management can be targeted at the most critical production sites and consumers since if on the one hand TNCs disproportionately influence the planet's climate and ecosystem<sup>19</sup>, on the other hand, they could become active agents of systemic change towards sustainable production ecosystem<sup>19,22,23</sup>. While efforts to engage TNCs in reducing CO<sub>2</sub> emissions and preserving ocean biodiversity achieved their first results<sup>20,24,25</sup>, a water footprint assessment of TNCs in the agricultural system is still missing and crucial to foster actions.

Here, we fill these two knowledge gaps by focusing on the emblematic case of the Brazilian soy to explore the magnitude of TNCs' dominance in the VWT and the major challenges to shifting toward corporate water stewardship in the food system. To this aim, we capitalize on recent leading improvements in supply chain mapping by TRASE<sup>26,27</sup>, which releases highly resolute data of trade between the producer localities, the trader companies, and the importing countries. We estimate both green and blue soy uWF at the municipality scale using the most up-to-date data on land management, soil properties, and hydrological data. We focus on the case of Brazilian soy since the wide extension of the Brazilian territory spots the light on the importance of considering the sub-national ecological and climatic characteristics in the VWT assessment between countries<sup>18,28</sup>. Indeed, Brazil is one of the richest biodiversity countries in the world with six unique biomes<sup>29</sup> which, depending on their characteristics, possess large carbon stocks in their forests and soils, the largest global reserves of freshwater<sup>30</sup>, biodiversity hotspots<sup>31</sup>, and additionally regulate the water vapour fluxes to areas downwind<sup>32</sup> as well as the water stream flow<sup>33</sup>. At the same time, these biomes support the largest soy production worldwide (122 million tons in 2020)<sup>34</sup>, handled by

some of the biggest TNCs worldwide<sup>35</sup>. The ecological peculiarities of the biomes are threatened by the soy harvesting extensification<sup>36,37</sup> (+163% from 2000 to 2019)<sup>34</sup>. Also, the choice of Brazil offers an example of a country which would benefit from a TNCs' corporate activity when the local authority defects in planning a water resources management<sup>38</sup>, thus exacerbating water shortages<sup>39</sup>. Further, Brazilian soy harvest is emblematic due to the interactions between land use change, the alteration of the hydrological cycle<sup>40–42</sup>, and climate change which, all together turn into more frequent droughts<sup>43</sup>, water competition and water grabbing<sup>44</sup>, evidencing the unfeasibility to sustain the soy production as has been pursued so far. The key point in involving TNCs in the VWT assessment is to allow them to cope with finding synergies between business and environmental conservation: their role to avoid climatic and ecological tipping points is increasingly perceived as fundamental<sup>38,45</sup> and, at the same time, their ultimate dependency on the integrity of the hydrological cycle to maintain their profit is growing evidence<sup>46</sup>.

## Results

**Single TNCs displace more VW than single countries.** Spatially explicit VW flows linking local production sites with supply chain actors (traders and importers) help guide efforts to boost sustainable water use and mitigate risk propagation in the global production ecosystem. The VW flows shown in Fig. 1 disentangle the complex interplay between producing municipalities, TNCs and importing countries within the Brazilian soy VW export. VW flows depart from 1620 traced municipalities in Brazil and reach the top-10 importing countries selected in this study (see Methods). By associating each VW flow directed to one of the ten importers with a dominant TNC, we were able to highlight the top-nine companies that manage the 4429 VW flows connecting producing municipalities to the importers (i.e. a single municipality can source more than one country and eventually more than one company). In 2018, these top TNCs handled around 100 billion m<sup>3</sup> of VW (around 70% of the total VW flow) corresponding to an average of 7 million m<sup>3</sup> virtually departing from each municipality (Fig. 1). The share of the top-10 importers is dominated by China (80 Gm<sup>3</sup>, 80%), followed by Netherlands (5 Gm<sup>3</sup>, 5%), South Korea and Spain (3 Gm<sup>3</sup>, 3%). Among these top importers, China is the biggest actor both among countries and companies because it depends on imports for 90% of its total soy supply<sup>47</sup>. The VW flow imported by a single country is typically handled by a minimum of 3 (United Kingdom, where Cargill shows a net dominance with respect to the other TNCs) to a maximum of 7 (Italy, Thailand) different traders among the dominant companies (Fig. 1). Considering the top-4 companies, we find nearly equal power in trading around 10–15% of the total VW volume: Bunge (15 Gm<sup>3</sup>, 14%), Cargill (14 Gm<sup>3</sup>, 14%), ADM (12 Gm<sup>3</sup>, 11%), and Louis Dreyfus (11 Gm<sup>3</sup>, 10%) dominate the VW export toward the top-10 importers (Supplementary Fig. 1).

The key finding of this analysis is that the VW exchanged by the biggest companies is greater than that displaced by countries, except for China. In 2018, Bunge displaced more than three times the VW volume imported by Thailand (4 Gm<sup>3</sup>), the second major Asian soy importer after China, and Louis Dreyfus displaced more than twice the VW of the Netherlands (5 Gm<sup>3</sup>), which is the largest European importer (Supplementary Fig. 1).

The role played by companies in displacing such volumes of VW highlights the importance for companies to engage in a form of corporate water stewardship—as part of the biosphere stewardship<sup>19</sup>—to ensure sustainable targets of production and water management in the food system. The disentangled network in Fig. 1 shows how countries are necessarily tied to companies in

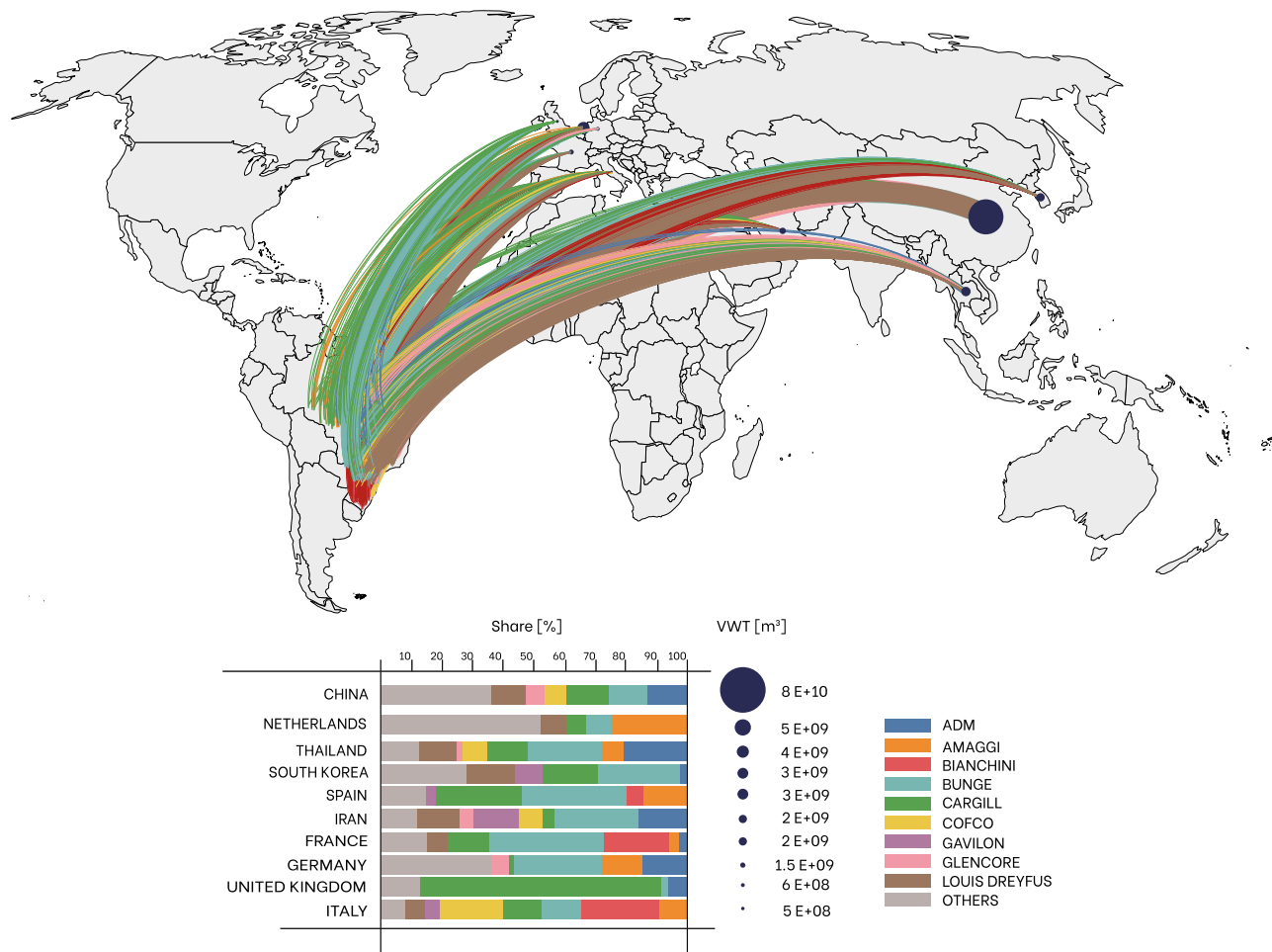


**Fig. 1 Spatially explicit virtual water flows linking local production sites with traders and importers.** Sub-national and company-specific virtual water flows ( $m^3$ ) of soybean products from Brazilian municipalities to top importer countries in 2018. The bubble size on the map represents for each country the total traced incoming virtual water volume from all the exporting companies. The colours and the size of the edges identify the trading company and the weight of each virtual water flow leaving the Brazilian municipality. Only the edges associated with the top-nine trading companies are shown. The bottom legend shows also the companies' share of the total virtual water import by each country in 2018.

their intent to meet supply-chain sustainable goals and thus they should dialogue with them to reach sustainable local productions. In the same way, companies are the connecting dowel with local production, and, when well established in a producing country, they can even go as far as lobbying local governments for additional support to drive innovation<sup>38</sup>.

**TNCs and countries have different uWFs.** We now group municipalities according to the top 10 countries of import and the TNCs that they source with virtual water (Fig. 2). Results show a heterogeneous water footprint across Brazil. The uWF of importing countries shows smaller variability compared to that of companies: from a minimum of  $1340 m^3/ton$  (Germany) to a maximum of  $1560 m^3/ton$  (Italy) versus  $1350 m^3/ton$  (Louis Dreyfus) to  $1800 m^3/ton$  (Gavilon). Hence, importers can average out their uWF thanks to their chance of sourcing from a heterogeneous basket of companies displaced across the Brazilian country.

Among top importers, Germany (average uWF of  $1340 m^3/ton$ ), South Korea ( $1410 m^3/ton$ ), and France ( $1430 m^3/ton$ ) (Supplementary Table 1) show the largest uWF variability, as shown by the 25th–75th percentile ( $1000$ – $1550 m^3/ton$ ) in Fig. 2a. The whiskers of South Korea, France, and Italy highlight high uWFs where yields

show minimum peaks, mainly in the Southernmost municipalities (Supplementary Fig. 2).

Among companies, Bianchini and Gavilon (Fig. 2b) show the widest range of uWF values with the 90th percentiles exceeding  $2400 m^3/ton$ . The highest uWF values of Bianchini and Gavilon are found in the municipalities of Sant'Ana do Livramento ( $3850 m^3/ton$ ) and Sentinela do Sul ( $4718 m^3/ton$ ) in Rio Grande do Sul state (Supplementary Fig. 2).

Overall, VW flows originate from climatically and agronomically heterogeneous sites in Brazil. This sub-national strong heterogeneity exposes producers and, thus, companies and importing countries to different water footprints (Supplementary Figs. 4 and 5) and drought probability (see 'Methods'). Bianchini, COFCO, ADM, and Louis Dreyfus are the most exposed actors to drought events with a probability of occurrence around 25%, while Amaggi is the least exposed company, but it still shows a probability of 14% (Supplementary Table 2).

The VW flows-weighted barycenters (Fig. 2) show that the Cerrado tropical savanna is the region where both countries' and companies' water footprints are predominantly located. However, while those of countries are all located in this biome, those of companies are more heterogeneously distributed across the country (Fig. 2d). Gavilon, Louis Dreyfus, and Bianchini are located in Mata Atlantica and at the edge between this one and

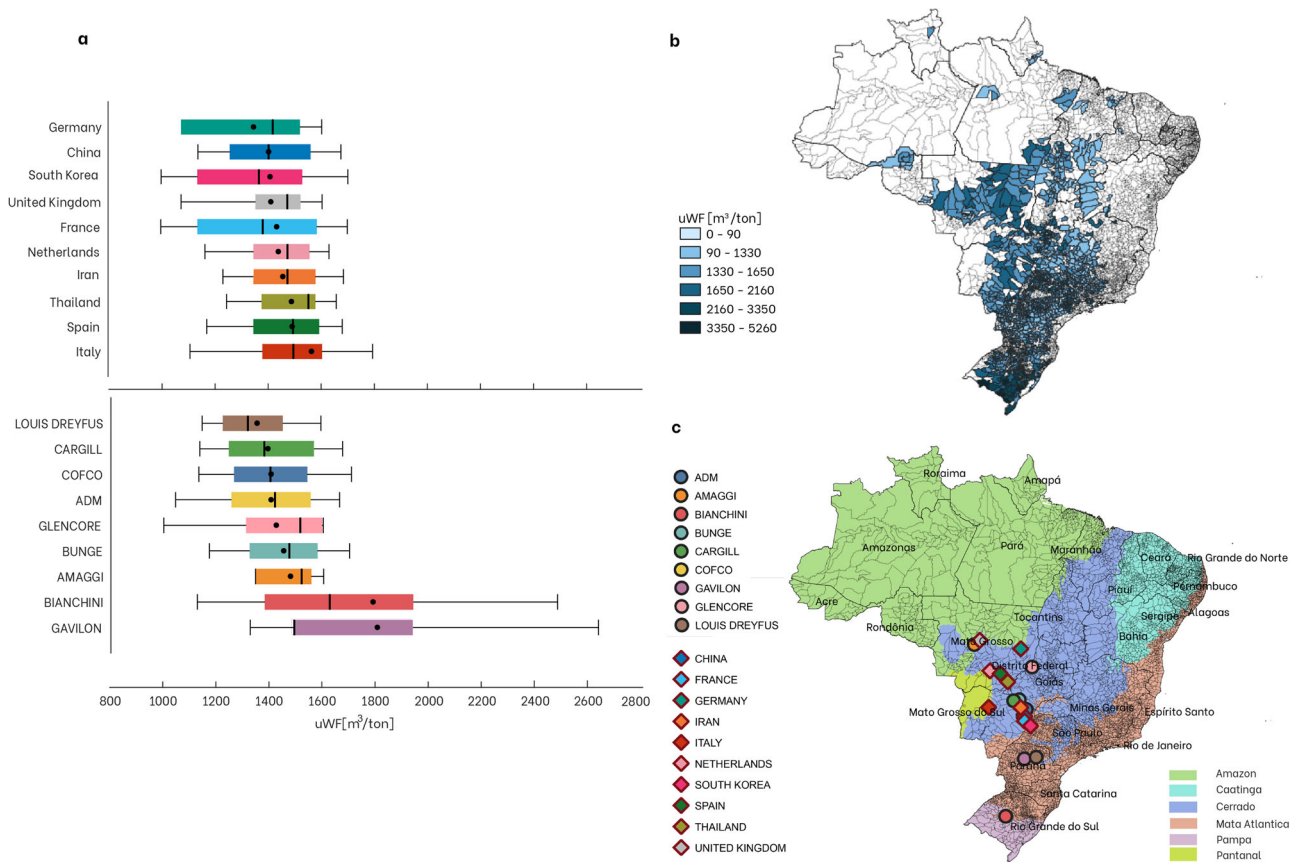


**Fig. 2** The different unit water footprint of trading companies and countries. **a** Boxplots of the unit water footprint (uWF, m<sup>3</sup>/ton) of soybean production for the top-ten importers in 2018 and the top-nine dominant trading companies. The left and the right whiskers refer to 10th- and 90th-percentile, respectively, while the dot represents the average uWF. **b** Sub-national uWF of soybean in the active exporting municipalities in 2018. **c** Virtual water-weighted barycenters of countries' and trading companies' virtual water trade over the Brazilian biomes in 2018.

the Brazilian Pampa. In this Southernmost biome, and especially in the state of Rio Grande do Sul (the most irrigated state of the country<sup>48</sup>), ET rates, uWF values and drought probability at the municipality scale are among the highest in Brazil. Differently, thanks to high yields, companies extending their sourcing toward the Amazon biome show low uWFs, but there the deforestation indirectly impacts the hydrological cycle, thus threatening the soil moisture availability for agriculture<sup>5,39,41</sup>. The sub-national heterogeneity of companies' uWF distribution provides evidence of different climatic threats and water-use issues companies have to face and manage. The sub-national distribution of VW flows barycenters we show (Fig. 2) can strongly enhance the effectiveness of VW flows assessment and provide a tool for the importing countries to know, and manage, their food supply chain through cooperation with traders.

**Managing delocalized water footprint.** The high-resolution VW flows assessment provided in this study allows country-specific analyses and ad hoc re-connection of the importer to the delocalized production sites and the associated footprint on water resources. By zooming in on a single importer country, we highlight for the first time the keystone role of TNCs in trading virtual water and, thus, indirectly the power to manage water resources. As an example, we focus on Italy that, along with Thailand, is sourced by the widest basket of companies (7) (Fig. 1). In 2018 Italy imported 430 million m<sup>3</sup> through these 7 companies, over a total volume of 468 million m<sup>3</sup>. The dominant company for the Italian VW import is Bianchini, handling 120 million m<sup>3</sup>, followed by COFCO (96 million m<sup>3</sup>), and Cargill

(60 million m<sup>3</sup>). Around 40% of the volume traded by the seven companies comes from ten municipalities only (Fig. 3). Among these municipalities, Sant'Ana do Livramento and Rio Pardo in Rio Grande do Sul—which export through Bianchini—show the highest uWF values (3850 and 2480 m<sup>3</sup>/ton, respectively) while Santa Bárbara do Sul (Bianchini) and Cláudia in Mato Grosso (Cargill) have the highest drought probability (30%).

Results demonstrate that the agro-climatical heterogeneity and the diverse rate of production make the water footprint of companies at the municipality scale vary a lot and expose both the companies and the importer country to specific climatic threats. Indeed, Italy shows the highest uWF among importing countries (1560 m<sup>3</sup>/ton), thus requiring more water per kilogram of cultivated soy, because it imports primarily from Bianchini (1790 m<sup>3</sup>/ton) and additionally from Gavilon (1800 m<sup>3</sup>/ton). However, even though Bianchini is exposed to a 26% of drought probability and COFCO (the second Italian supplier) is exposed to a 25% of drought probability, Italy shows a little lower climatic exposure to drought (around 23%), thanks to its chance of sourcing from a heterogeneous basket of companies. In other words, while companies can temper their level of exposure by diversifying the municipalities they source from, countries have an extra degree of freedom (and therefore possibly less exposure) by being also able to diversify across different companies.

**VWT is increasing despite decreasing uWFs.** The total VW flow from the traced municipalities to the top-10 importers increased from 43 billion m<sup>3</sup> to about 100 billion m<sup>3</sup> (+133%) over the

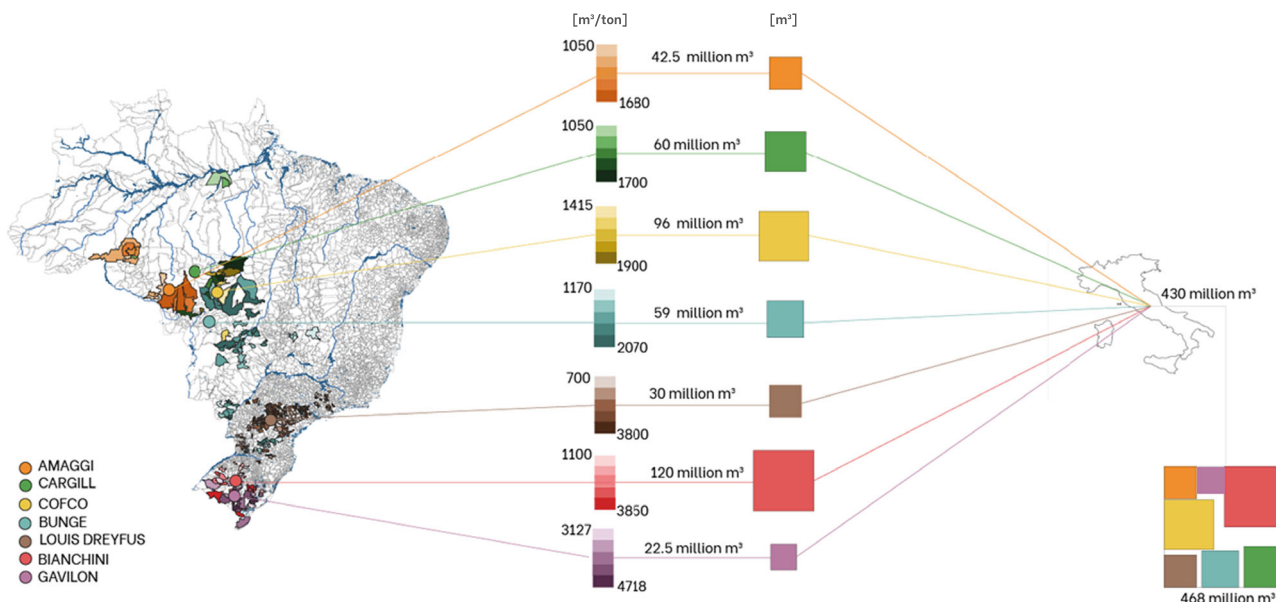


**Fig. 3 Tripartite network of the virtual water flows (m<sup>3</sup>) at the company's scale from Brazilian municipalities to Italy in 2018.** The map reports the unitary water footprint (uWF) at the company's scale over the Brazilian territory (layer 1). The links depart from the VW weighted barycenters of production of each company and reach their range of uWFs (m<sup>3</sup>/ton) and their total exported volume (m<sup>3</sup>) (layer 2). A unique colour scale is used for each company, the minimum and maximum values of uWF are shown in the first column and their VW export to Italy in the second column of layer 2. Finally, each VW flow is connected to Italy (layer 3). The hierarchies of the companies are aggregated in the treemap, where the empty space accounts for rest of the companies that trade to Italy.

period 2004–2018, due to both the establishment of 1230 new connections and an intensification (+44%) of the average VW flow traded over a single connection. Looking at the geography of soybean producers (Fig. 4a), the production growth was dominated by a process of extensification, with the appearance of 602 new municipalities (Fig. 4b), which were not active in the soybean market in 2004. At the same time, our results show a significant intensification of production over stable municipalities and a consequent increment of water demand by 48 million m<sup>3</sup> (Fig. 4c). In particular, the municipality of Sorriso, the core of the Brazilian soybean production in Mato Grosso, increased its VW flow from 185 million m<sup>3</sup> up to 2.3 billion m<sup>3</sup> (Fig. 4c). Notably, the annual VW flow departing from Sorriso (Fig. 4a) and reaching all top-ten study importers corresponds to nearly the VW import of South Korea in 2018, sourcing 7 of the 9 dominant companies (all except for Louis Dreyfus and Bianchini). Sorriso increased its agricultural efficiency by 24% (reaching 3.7 ton/ha in 2018), thanks to the enhancement of soy crop yields in the last decade. Indeed, despite the growth of VW flows, the average uWF decreased by 40% on average—from 2566 to 1553 m<sup>3</sup>/ton—thanks to a yield increasing from 2.2 to 3.3 ton/ha (+36%).

Among the new exporting municipalities, the top 30 ones account in 2018 for 10% of the total traced VW flow, which mostly departs from the Central region of Brazil (Fig. 4b). This recent pattern of extensification should raise concern and boost improved water management; in fact, this region results prone to droughts (Supplementary Fig. 2) and to water stress, as has been recently testified by e.g. GRACE satellites which registered in 2021 a terrestrial water depletion between 200 to 500 mm over this Central region<sup>39</sup>. Our results show also that on average TNCs enlarged their VW flows and consolidated their dominance in the Brazilian soy VW trade. However, new (COFCO) or smallest (Gavilon) companies acquired more significance in the VW export. COFCO, in 2018 is already the fifth VW exporter, replacing Amaggi which instead decremented its VW export by 22% in 2018. In 2004 the largest VW flows were exported by

Bunge, Cargill, ADM, and Bianchini. Among them ADM, Cargill and Bianchini show the most relevant variation; ADM and Cargill tripled their VW export while Bianchini—which shows the highest yield increment (+123%) and uWF decrement (−61%) among the top 9 exporters—lowered its VW export by 22%. In 2004, it was the fourth VW exporter and in 2018 it was displaced by Louis Dreyfus which, although showing a yield increment of 42% and a uWF decrement of 30%, in 2018 exported 7 times more virtual water than in 2004. Overall, we observe an intensification of many soy producers in climatically vulnerable sites. In fact, VW flows newly originated from the North East Cerrado at the intersection of Maranhão, Tocantins, Piauí and Bahia, which are some of the driest states in Brazil (Supplementary Fig. 2). Despite these patterns, the range of weighted drought probability shifted from 19–29% (2004) to 21–24% (2018) for importing countries (Supplementary Table 1) and from 14–35% (2004) to 14–26% (2018) for companies (Supplementary Table 2). The reason behind the average decrease in drought exposure lies in the expansion toward less dry municipalities. Between 2004 and 2018 new VW flows departed from the cleared land in the Amazon (from the state of Rondônia) while other flows consolidated in the Western part of Cerrado, in Mato Grosso (Fig. 4b and Supplementary Fig. 2). In the short term, the shift has allowed a decrement in drought exposure. However, we acknowledge that in the long term, the increased deforestation in this biome and the related biodiversity loss may cause knock-on effects on the hydrological regime and local water availability. The virtual water network at study in the year 2004 is available in the online repository <https://doi.org/10.5281/zenodo.7334623>. To catch the magnitude of the soy water footprint increase in Brazil between 2004 and 2018, we can compare it with that of coffee, an important cash crop exported worldwide, which—differently from soy—decreased its total WF by 16% from 2004 to 2016. Indeed, despite coffee having an uWF (6110 l/kg) 3 times higher than soy (1830 l/kg), in 2016 its production accounted for a 9.5 times lower WF volume (185 Gm<sup>3</sup> versus 1800 Gm<sup>3</sup>)<sup>14</sup>.

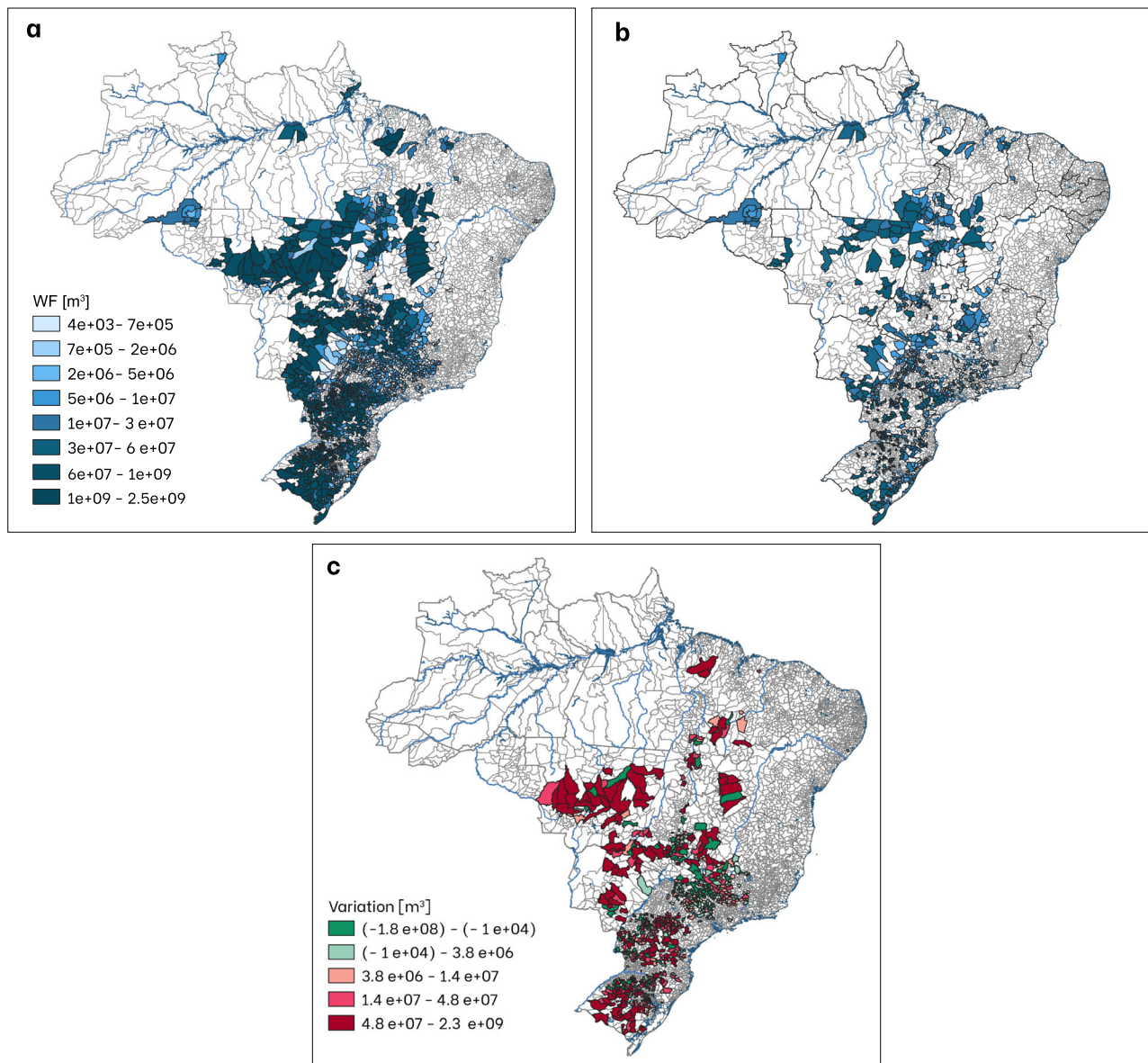


**Fig. 4** Virtual water export of soy toward top ten importing countries between 2004 and 2018. **a** Virtual water import (WF,  $\text{m}^3$ ) of production associated with the primary and processed soy export departing from each municipality and directed to the top-10 importers in 2018. **b** New municipalities involved in the virtual water export to the top-10 importers. These municipalities were not operating in 2004, but they become active during the period 2004–2018. **c** Changes in the virtual water export between 2004 and 2018 over stable municipalities. Green (magenta) colours identify a decrease (increase) in the virtual water export. The main rivers are also shown.

## Discussion

Transnational corporations are emerging as critical players in global water governance to enhance water use sustainability<sup>21</sup>. In this study, we highlight the role of TNCs in the virtual water flows connecting Brazil to the top 10 importers of soybean over the period 2004–2018. We disentangle the 10 country-scale VW flows typically analysed in the literature into 4429 sites—and company-specific—flows handled by the top-9 traders in the global soy market (Fig. 1 and Supplementary Fig. 1). This assessment sheds light on the 1620 (1018) Brazilian municipalities where the top-ten global importers of soy delocalize their water footprint (Fig. 1) in 2018 (in 2004). We thus provide a novel and useful tool to improve the supply chain sustainability governance<sup>26,49,50</sup> in terms of water use and stakeholders' involvement<sup>18</sup> in the process of enhancing water use sustainability. With this study, we demonstrate that companies can take the lead in modifying and

improving the VW supply chain<sup>19</sup>; e.g. in 2018, Bunge displaced almost four times the VW volume imported by Thailand ( $4 \text{ Gm}^3$ ), and Louis Dreyfus displaced more than twice the VW of the Netherlands ( $5 \text{ Gm}^3$ ). Cargill ( $14 \text{ Gm}^3$ ) and ADM ( $12 \text{ Gm}^3$ ) are the other dominant VW traders among the nine analysed in this study.

Although governmental policies are essential<sup>23</sup> to achieve sustainable supply chains, our results show how countries are necessarily subjected to companies when dealing with their outsourced pressure on (far) water resources. Companies' choices about where to buy soybean shape importers' final water footprint (Fig. 2). The puzzle of municipalities sourcing soybean to each company is also a driver of the water risk—i.e. drought probability in this study—associated with their business and the whole supply chain vulnerability. If, on the one hand, companies and countries are already engaged in deforestation commitments, e.g.

the Amsterdam Declarations Partnerships<sup>51</sup>, on the other hand, they face increasing drought occurrence<sup>39,43</sup> and, when they succeed in preserving high-deforestation risk sites, they can still incur in high water footprint (e.g. Gaviion vs Louis Dreyfus) or drought occurrence (e.g. Amaggi vs Bianchini). This is also confirmed by the IPCC 2022 final report that estimates Brazil as highly vulnerable to drought due to a combination of social, economic, and infrastructural factors<sup>52</sup>. This issue should warn both the TNCs operating in Brazil and the importing countries. Estimates indicate that more than 44% of the EU agricultural imports from the global market will become highly vulnerable to drought in the future because of climate change<sup>53</sup>. In particular, the drought exposure of the EU agricultural imports from Brazil will increase by 35% by 2050<sup>53</sup>, thus showing the relevance of better-targeted food reserves to cope with the climate variability<sup>54</sup>.

Putting our study in the context of the UN Sustainable Development Goals, we acknowledge that possible competition or trade-offs can arise for companies and countries when simultaneously tackling diverse aspects of sustainability: e.g., actions for land and biodiversity (SDG 15), climate (SDG 12), and water conservation (SDG 6). We found that companies associated with higher CO<sub>2</sub> emissions<sup>55</sup> and biodiversity loss<sup>56</sup> show lower uWF (e.g., Amaggi, Cargill, ADM—uWF of about 1400 m<sup>3</sup>/tons) compared to companies operating in the Southernmost region (e.g., Bianchini and Gaviion—uWF of about 1800 m<sup>3</sup>/tons). Interdependencies between climate change, deforestation, droughts, land-use change and biodiversity loss<sup>57–60</sup> should thus be considered together in future studies to provide TNCs with information on the synergies and trade-offs associated with their actions. Finally, competition for water use among different sectors (especially in areas where irrigation, hydroelectric power generation, and household demand compete for the same water supply, e.g. in the Rio Sao Francisco’s tributaries basins in Western Bahia<sup>44</sup>) poses a further challenge for the Brazilian water management, which should be considered.

To address this multi-target challenge of sustainable water management, we propose a perspective corporate initiative (summarized in Fig. 5), where TNCs are the pivotal node to provide Science with detailed data to reconstruct high-resolution VW trade and WF assessment. To accomplish this, science should engage and connect companies and countries through a collaborative process, mutual peer monitoring, and increased fairness in the data declaration thanks to robust water footprint assessment. Thanks to this assessment, on the one hand, companies can protect their core activity from water risks while reducing their pressure on water resources. On the other hand, countries can take advantage of a more detailed water footprint and risk assessment to optimize their total supply. In this way, countries are capable to design more effective and targeted water policies for both imports and domestic production. This mutual collaboration additionally provides detailed information for consumers (e.g. water footprint labels) that turn into more sustainable patterns of consumption and active societal awareness. We frame for each actor of the initiative the main actions implementable and the main tools available, thanks to the collaboration with another actor of the process (Fig. 5). For example, Science receives detailed trade data from TNCs, thus becoming able to assess their water footprint. In return, TNCs receive useful data on the water risk and footprint associated with their activity. With this information, TNCs can lead the corporate initiative and promote sustainable targets that in turn can boost governmental policies and societal awareness. The actions applied and the tool provided by each actor finally lead to the two key aims of the collaborative process: the conservation of water resources and the security of

food supply chains, broadening the biosphere stewardship initiative to water resources in the food system.

Our study offers a new perspective on water management and provides new data and tools to develop solutions for water preservation in the context of the complex sustainability framework that companies and countries should embrace in a joint effort with the need to put water at the heart of public and private governance<sup>52</sup>.

## Methods

### Trade data sources and pre-processing

**Countries selection from FAOSTAT.** To select the major importing countries of Brazilian soy in the time interval (2004–2018), we focused on the exchanged tons of primary soybean, soybean oil and soybean cake exported by Brazil between 2004 and 2018, from the FAO import-export detailed matrices<sup>61</sup>. We transformed each secondary item (soybean oil and soybean cake) flows into its primary soy equivalent—according to available conversion factors<sup>62</sup> (Supplementary Table 3)—in order to properly sum the export of the three items. We then cumulated the total imported tons for each importing country from 2004 to 2018 (once transformed into equivalent soybean tons) and we obtained the top-ten importers over these years, i.e. China, Netherlands, Spain, France, Thailand, Germany, South Korea, Iran, Italy and United Kingdom.

**Sub-national and TNC’s trade data from TRASE.** To focus on the major TNCs which handle the soy flows of top importing countries, we sourced high spatial resolution data of production and harvested areas at the sub-national scale—where municipalities are related to exporter hubs, traders, and importer countries—from the Trase initiative database<sup>27</sup>, developed for tracking the supply chains of commodities exposed to deforestation risk<sup>63</sup>. From this dataset, we selected the Brazilian soy export between 2004 and 2018 of the ten previously selected countries. We obtained trade matrices reporting, for each country, the municipalities along the rows and the trading companies along the columns. Over the 297 companies trading Brazilian soybean toward the ten selected countries, we considered the major nine, which cover at least 80% of the trade of each country at study. For each selected country, we organized from the Trase dataset a trade matrix  $M_{c,t}(i, comp)$ , where  $c$  is the importing country in the year  $t$ ,  $i$  is the producing municipality and  $comp$  the TNC handling the export. The matrix  $M$  is organized as follows: the municipalities involved in the production (identified by their geographical code) are reported in the rows while the columns refer to companies. Moreover, we organized a comprehensive vector of geographical codes  $G_c(t)$ , a vector of harvested areas  $A_c(t)$ , a vector of produced soy equivalent tonnes  $T_c(t)$ , where  $i$  is a producer municipality in the study year  $t$  (respectively, 2004 and 2018). Finally, the municipalities’ longitudes and latitudes were collected in corresponding vectors.

**Comparative analysis.** We compare the imported tons of major importing countries at study reported by FAO<sup>61</sup> and by the Trase for the period 2004–2018. Since the comparison between FAO and TRASE data is assessed for each country one by one, the dimension of the sample is unitary (the single import of a country  $c$  in a year  $t$  recorded by FAO,  $T_{FaO,c,t}$  or Trase,  $T_{Trase,c,t}$ ). Assuming that the mean of  $T_{FaO,c,t}$  is the reference value recorded by Trase  $T_{Trase,c,t}$ , the squared deviation  $s_{trade,c,t}^2$  associated with the import of a country  $c$  in a year  $t$  reads as:

$$s_{trade,c,t}^2 = (T_{FaO,c,t} - T_{Trase,c,t})^2 \tag{1}$$

being:

$$\sigma_{trade,c,t} = \sqrt{s_{trade,c,t}^2} = \sqrt{(T_{FaO,c,t} - T_{Trase,c,t})^2} \tag{2}$$

We are able to define the variation between the two trade datasets for each country  $c$  in a year  $t$  by means of a coefficient of variation  $CV_{c,trade,t}$  for each year  $t$  between 2004 and 2018, namely:

$$CV_{trade,c,t} = \frac{\sigma}{T_{Trase,c,t}} = \frac{\sqrt{(T_{FaO,c,t} - T_{Trase,c,t})^2}}{T_{Trase,c,t}} = \frac{|(T_{FaO,c,t} - T_{Trase,c,t})|}{T_{Trase,c,t}} \tag{3}$$

We perform the analysis for every year from 2004 to 2018 for each of the 10 importing countries at study, as reported in Supplementary Fig. 6.

We then calculate the mean  $CV_{trade,c}$  in the time interval for each country as:

$$CV_{trade,c} = \frac{\sum_{t=1}^{Years} CV_{trade,c,t} \cdot T_{FaO,c,t}}{\sum_{t=1}^{Years} T_{FaO,c,t}} \tag{4}$$

where Years is the number of years between 2004 and 2018.

We then find an overall mean weighted variation ( $CV_{trade}$ ) between the two dataset from 2004 to 2018 considering the ten importing countries of 5%,

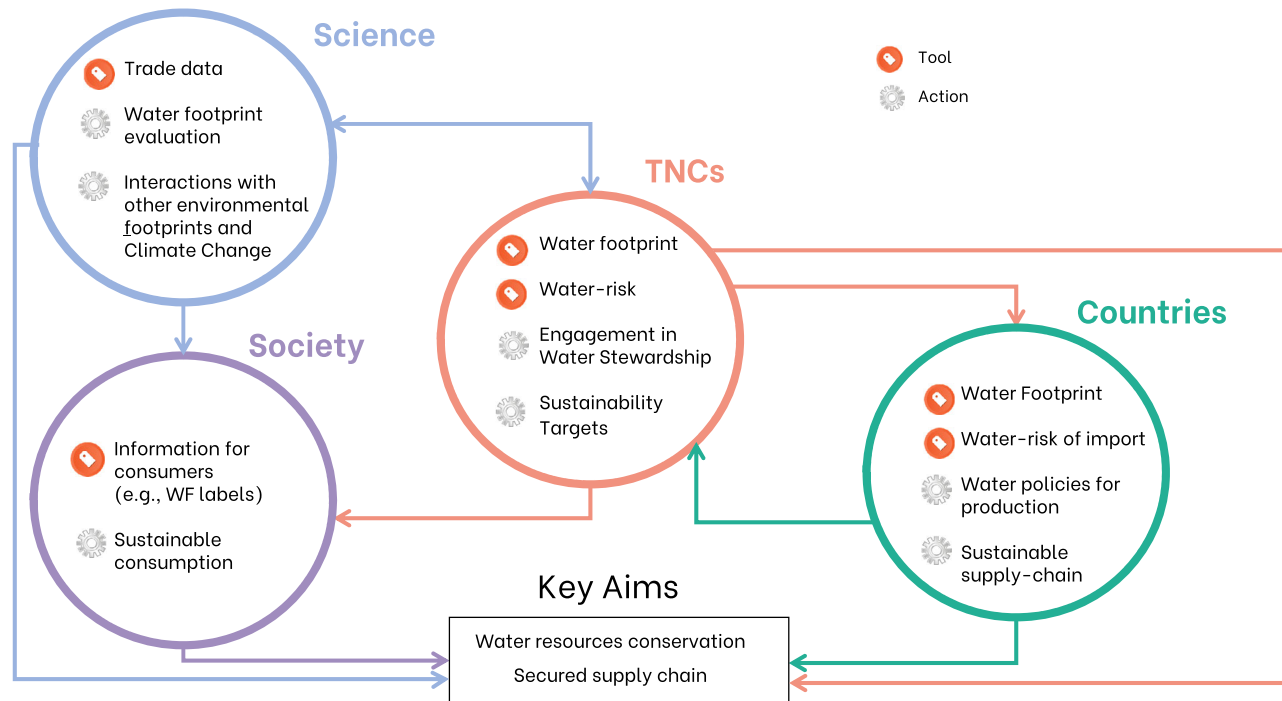


**Fig. 5 A water stewardship perspective to sustain the conservation of water resources and secure food supply chains.** Inter-relationships between science, TNCs, countries and society to synergically sustain the conservation of water resources and secure food supply chains. We frame for each actor the main actions implementable and the main tools available, thanks to the collaboration with another actor of the initiative. For example, Science receives detailed trade data from TNCs, thus assessing their water footprint. In return, TNCs receive useful data on the water risk associated to their activity. With this information, TNCs can lead the corporate initiative and promote sustainable targets that in turn can boost governmental policies and societal awareness. Considering the larger amount of virtual water displaced on average by single TNCs with respect to single countries, and their transnational operational range, TNCs are identified as the pivotal layer in the virtual water trade that can broaden the biosphere stewardship initiative to water resources in the food system.

calculated as:

$$CV_{\text{trade}} = \frac{\sum_{c=1}^C CV_{\text{trade},c} \cdot T_{\text{Fao},c}}{\sum_{c=1}^C T_{\text{Fao},c}} \quad (5)$$

Where  $C$  is the total number of importing countries at study.

**Evaluation of soy uWF.** In the present study, the uWF of soy, uWF, in a generic producer municipality  $i$  in year  $t$  is defined as the ratio between the total volume of water evapotranspired during the growing season in year  $t$ ,  $ETA(t)$  (mm), and the crop actual yield  $Y(t)$ ; namely:

$$uWF_i(t) = 10 \cdot \frac{ETA_i(t)}{Y_i(t)} \left[ \frac{\text{m}^3}{\text{ton}} \right] \quad (6)$$

where the factor 10 converts the evapotranspired water height expressed in mm into a water volume per land surface expressed in  $\text{m}^3/\text{ha}$ . Depending on agricultural practices, climate and soil properties, the crop evapotranspires green (i.e. precipitation water stored in the (top of) soil and vegetation) and blue (i.e. irrigation water withdrawn from surface and ground water bodies) water. In this study, we assess both green and blue actual evapotranspiration, in both rainfed or irrigated conditions, obtaining both blue and green uWF $_i$  (Supplementary Fig. 7). The total uWF in a generic producer municipality  $i$  in a year  $t$  is calculated as the sum of the green and blue components:

$$uWF_i(t) = uWF_i^g(t) + uWF_i^b(t) \left[ \frac{\text{m}^3}{\text{ton}} \right] \quad (7)$$

**Crop actual yield.** We calculate the crop actual yield  $Y_i(t)$  in a given year at the municipality scale, (ton/ha) as:

$$Y_i(t) = \frac{T_i(t)}{A_i(t)}, \left[ \frac{\text{ton}}{\text{ha}} \right] \quad (8)$$

where  $T$  is the total soybean production at the municipality scale and  $A$  is the total (rainfed plus irrigated) harvested area.

**Crop evapotranspiration.** The model described in the following is run at a pixel level, with a spatial resolution of  $5 \times 5$  arc min; gridded values are then aggregated

at the municipality scale to determine the actual evapotranspiration  $ETA$  in a producer municipality  $i$  over a year  $t$ .

The  $ETA$  of a crop in a year  $t$  is the water evapotranspired by the crop in non-standard conditions (diseases and water stress can occur during the growth). It is calculated as the sum over the year of the  $ETA$  in one or more growing seasons (i.e.,  $ETA_{LGP}$ ). The  $ETA_{LGP}$  is obtained by summing up over the length of the growing periods (LGP) the daily actual evapotranspiration,  $ETA_j$  (mm/d), i.e.,

$$ETA_{LGP} = \sum_{j=1}^{LGP} ETA_j \left[ \frac{\text{mm}}{\text{LGP}} \right] \quad (9)$$

with  $j$  indicating the day of the growing period. LGP is delimited by the planting and harvesting dates taken from Portmann et al.<sup>64</sup>. Following the well-established procedure introduced by Allen et al.<sup>65</sup>, we estimate the daily evapotranspiration  $ETA_j$  as:

$$ETA_j = ET0_j \cdot k_{c,j} \cdot k_{s,j} \left[ \frac{\text{mm}}{\text{d}} \right] \quad (10)$$

where  $ET0_j$  is the daily reference evapotranspiration (mm/d) from a hypothetical well-watered grass surface with fixed crop height, albedo and canopy resistance,  $k_{c,j}$  is the daily crop coefficient, and  $k_{s,j}$  is the daily water stress coefficient depending on the available soil water content, with a value between 0 (maximum water stress) and 1 (no water stress). The  $ET0$  quantifies the reference evapotranspiration, depending only on climate conditions such as temperature, humidity, solar radiation and wind velocity. Gridded monthly long-term average reference evapotranspiration data  $ET0_m$  at  $10 \times 10$  arc min resolution are sourced by Version 4 of the CRU TS climate dataset<sup>66</sup>. These data are converted to  $5 \times 5$  arc min data by subdividing each grid cell into four square elements and assigning them the corresponding  $10 \times 10$  arc values. Daily  $ET0_j$  values are determined through a linear interpolation of monthly climatic data and attributing the monthly  $ET0_m$  value to the middle of the month<sup>67</sup>. The crop coefficient,  $k_{c,j}$ , is the percentage of evapotranspiration of the specific crop, with respect to the  $ET0$  of the standard surface. It depends on crop characteristics and, to a limited extent, on climate. It is influenced by crop height, albedo, canopy resistance, and evaporation from bare soil. During the growing period,  $k_{c,j}$  varies with a characteristic shape divided into four growing stages (I: initial phase, II: development stage, III: midseason, and IV:

late season) of  $l_I, l_{II}, l_{III}$ , and  $l_{IV}$  days length, respectively, that reads

$$k_{c,j} = \begin{cases} k_{c,in} & j \in \text{I stage} \\ j \cdot \frac{k_{c,mid} - k_{c,in}}{j - l_I} & j \in \text{II stage} \\ k_{c,mid} & j \in \text{III stage} \\ j \cdot \frac{k_{c,i} - k_{c,mid}}{j - l_I - l_{II} - l_{III}} & j \in \text{IV stage} \end{cases} \quad (11)$$

We use values from Allen et al.<sup>65</sup> for the constants  $k_{c,in}$ ,  $k_{c,mid}$ , and  $k_{c,f}$ , while the length of each stage,  $l_{st}$ , is calculated as a fraction,  $\rho$ , of the length of the growing period ( $l_{st} = \rho_{st} \cdot LGP$ );  $\rho_{st}$  is defined for each stage (with  $st = I-IV$ ) according to Mekonnen and Hoekstra<sup>68</sup>, whose study provides specific values of  $\rho$  for different climatic regions. Lengths are rounded to the nearest integer and stage I is adjusted to guarantee the exact length of the growing period.

Since the daily  $k_{s,j}$  in Eq. (10) is different in rainfed or irrigated conditions, as well as the  $ET_0$ , (i.e. the growing period can have different planting dates in rainfed and irrigated conditions), we assess the daily  $ETA_j$  (green or blue), calculated with Eq. (10), in the two production types.

In rainfed conditions the total actual evapotranspiration  $ETA_R$  accounts only for the green water component  $ETA_R^g$ , being by definition  $ETA_R^b = 0$ . It depends on the soil moisture concentration, whose indicator is the water stress coefficient,  $k_{s,j}$ :

$$ETA_R = ET_R^g = k_{s,j} \cdot ETC \quad (12)$$

When rainfed,  $k_{s,j}$  varies as a function of soil moisture content, the field capacity and the rooting depth. To compute  $k_{s,j}$  daily value in rainfed conditions we follow the methodology detailed in Tuninetti et al.<sup>67</sup>. In the irrigated scenario water stress is avoided, thus  $k_{s,j} = 1$ . The  $ETA_I^g$  is calculated as in rainfed conditions, following Eq. (10). Note that  $ETA_I^g$  differs from  $ETA_R^g$  due to the different rooting depths. Indeed, rainfed crops tend to go deeper to exploit as much water as possible. Then, the  $ETA_I^b$  is evaluated as the amount of irrigation water required to fill the lack of rainfall:

$$ETA_I^b = ETC - ET_I^g \quad (13)$$

The overall evapotranspiration of green and blue water from a pixel,  $ETA_{LGP}^g$  and  $ETA_{LGP}^b$ , is the weighted mean of the rainfed and irrigated evapotranspiration:

$$ETA_{LGP}^g = \frac{ET_{R,LGP}^g \cdot A_R + ET_{I,LGP}^g \cdot A_I}{A_R + A_I} \quad (14)$$

$$ETA_{LGP}^b = \frac{ET_{I,LGP}^b \cdot A_I}{A_R + A_I} \quad (15)$$

where weights,  $A_R$  and  $A_I$ , are the crop-specific harvested areas distinguished between rainfed and irrigated production, For soy cultivation, according to Portman et al., we considered one growing period in a year  $t$ . The total  $ETA(t)$  in a can be thus calculated as:

$$ETA(t) = ETA^g(t) + ETA^b(t) \quad (16)$$

We run the model for the evaluation of  $ETA$  for both the years 2004 and 2018. We source global monthly irrigated and rainfed crop areas ( $A_R$  and  $A_I$ ) for 2004 from the MIRCA2000 dataset<sup>64</sup> calibrated around the year 2000; for 2018 from the irrigated areas provided by MapSPAM<sup>69</sup>, which refers to the year 2010. The yearly gridded values of  $ETA^g(t)$ ,  $ETA^b(t)$ , and total  $ETA(t)$  obtained with Eq. (9) are spatially averaged and re-gridded at the municipality scale to obtain the actual  $ETA_i(2004)$  and  $ETA_i(2018)$ . The green  $uWF_i^g(t)$  and blue  $uWF_i^b(t)$  in a generic producer municipality  $i$  in 2004 and 2018 are then calculated from Eq. (6), and the total  $uWF_i(t)$  eventually as the sum of green and blue components as in Eq. (7). In the exporting municipalities where the estimates of  $ETA_i(2004)$  and  $ETA_i(2018)$  were missed due to missing data on the irrigated and/or rainfed area or planting/harvesting dates, we estimated the  $ETA_i^g(t)$  and  $ETA_i^b(t)$  for 2004 and 2018 by associating the missing data with the  $ETA_i^g(t)$  and the  $ETA_i^b(t)$  of the closest municipality.

**Exposure to drought events.** To assess the climatic exposure of each exporting municipality  $i$  to drought, we calculate the probability of drought occurrence  $P_i$  by evaluating the frequency of a moderate to extreme dry anomaly occurring between January 1958 and December 2018 identified by the monthly self-calibrating Palmer Drought Severity Index (scPDSI)<sup>70</sup>; namely:

$$P_i = \frac{\sum_{m=1}^M \Theta(\text{scPDSI}_{i,m})}{M} \quad (17)$$

with:

$$\Theta(\text{scPDSI}_{i,m}) = \begin{cases} 1 & \text{if } \text{scPDSI}_{i,m} < -2 \\ 0 & \text{if } \text{scPDSI}_{i,m} \geq -2 \end{cases} \quad (18)$$

where  $\text{scPDSI}_{i,m}$  is the value of the scPDSI index in the  $i$ -th municipality in the  $m$ -th month between January 1958 and December 2018 and  $M$  is the total number of months within this period.

The scPDSI involves a classification of relative soil moisture conditions within 11 categories, which range from  $-4$  (extremely dry) to  $+4$  (extremely wet). The scPDSI index has been chosen because it is consistent with the climatic data of our study both in terms of methodology and data sources. In fact, it is based on a water-demand balance calculated using a water-budget system which involves local soil characteristics and historical records of precipitation and potential evapotranspiration (assessed as well by mean of the Penman–Monteith equation), which are the main input data for the water footprint assessment<sup>65</sup>. Moreover, climatic data are sourced from the CRU dataset<sup>66</sup>, consistently with our study. To assess the probability of drought associate with the VW import of a country or the VW export of a company (Supplementary Tables 2 and 3), the  $P_i$  from Eq. (17) of each municipality has been weighted with the volume of VW trade corresponding to the import country or the exporting company sourcing from the municipality  $i$ , over the VW volume of the related import or export.

**Sub-national VWT of countries and companies.** Once assessed the  $uWF_i(t)$  for each producer municipality through Eqs. (6) and (7), the VWT data were organized in a 3D matrix specific for a single year, as:

$$VWT_{i,comp,c}(t) = uWF_i(t) \cdot T_{i,comp,c}(t), \quad (19)$$

where  $i$  identifies the municipality, comp stands for the company which handles the flow, and  $c$  is the importer country. The virtual water import of a single country from a specific municipality reads

$$VWT_{i,c}^{\text{import}}(t) = \sum_{comp=1}^K VWT_{i,comp,c}(t) \quad (20)$$

where  $K$  is the total number of active companies trading virtual water for the country  $c$ . The VW import of a single country from all the municipalities it sources from reads

$$VWT_c^{\text{import}}(t) = \sum_{comp=1}^K \sum_{i=1}^I VWT_{i,comp,c}(t), \quad (21)$$

where  $I$  is the total number of exporting municipalities toward the importing country  $c$ . Analogously:

$$VWT_{i,comp}^{\text{export}}(t) = \sum_{c=1}^C VWT_{i,comp,c}(t), \quad (22)$$

where  $C$  is the total number of importing countries for an exporting company comp. The total VW export of a company reads

$$VWT_{comp}^{\text{export}}(t) = \sum_{c=1}^C \sum_{i=1}^I VWT_{i,comp,c}(t). \quad (23)$$

Among all companies (297 in 2018), we focused on the nine dominant TNCs which covered at least 80% of the total import (in tons, ref. 27) of the top-ten importer countries in 2018 and analyse their VWT also in 2004.

**Weighted barycenters.** Each importer country relies on a different basket of companies and sourcing municipalities, thus exhibiting a unique supply-chain network. To assess the average geographical production core sourcing each importer, we evaluate a weighted barycenter specific to each exporting company. For instance, in the case of Italy, we identify seven barycenters, one per each company. Hence, the country- and company-specific barycenters coordinates ( $b_{comp,c}^{x,y}(t)$ ) read

$$b_{comp,c}^x(t) = \frac{\sum_{i=1}^I \text{long}_i(t) \cdot VWT_{i,comp,c}(t)}{\sum_{i=1}^I VWT_{i,comp,c}(t)}, \quad (24)$$

$$b_{comp,c}^y(t) = \frac{\sum_{i=1}^I \text{lat}_i(t) \cdot VWT_{i,comp,c}(t)}{\sum_{i=1}^I VWT_{i,comp,c}(t)}, \quad (25)$$

where  $VWT_{i,comp,c}$  values are the weights used to obtain the average coordinates and represent the virtual water flow departing from each municipality  $i$ , handled by company comp, and reaching country  $c$ . We repeat this procedure for each company and country.

To find a unique barycenter for each country ( $b_c^{x,y}$ ), we average the company-specific barycenters, determined with Eq. (24), using the total virtual water trade handled by the company toward the study country as weight, namely

$$b_c^x(t) = \frac{\sum_{comp=1}^K [b_{comp,c}^x(t) \cdot \sum_{i=1}^I VWT_{i,comp,c}(t)]}{\sum_{comp=1}^K \sum_{i=1}^I VWT_{i,comp,c}(t)} \quad (26)$$

$$b_c^y(t) = \frac{\sum_{comp=1}^K [b_{comp,c}^y(t) \cdot \sum_{i=1}^I VWT_{i,comp,c}(t)]}{\sum_{comp=1}^K \sum_{i=1}^I VWT_{i,comp,c}(t)}. \quad (27)$$

Finally, we adopt the same approach as in Eqs. (26) and (27) to find out a unique barycenter for each company, namely

$$b_{comp}^x(t) = \frac{\sum_{c=1}^C [b_{comp,c}^x(t) \cdot \sum_{i=1}^I VWT_{i,c}(t)]}{\sum_{c=1}^C \sum_{i=1}^I VWT_{i,comp,c}(t)} \tag{28}$$

$$b_{comp}^y(t) = \frac{\sum_{c=1}^C [b_{comp,c}^y(t) \cdot \sum_{i=1}^I VWT_{i,comp,c}(t)]}{\sum_{c=1}^C \sum_{i=1}^I VWT_{i,comp,c}(t)} \tag{29}$$

**Error analysis.** The error on the uWF estimate and on the VWT assessment depends on the uncertainty related to their main components: yield ( $Y$ ), actual evapotranspiration (ETA) and trade ( $T$ ) according to their relations (see Eqs. (6) and (19)).

*Propagation of the uncertainty to the uWF.* According to the theory of error propagation, the uncertainty of the uWF reads as:

$$\begin{aligned} \sigma_{uWF}^2 &= \left(\frac{dU}{dY}\right)^2 \cdot \sigma_{ET}^2 + \left(\frac{dU}{dY}\right)^2 \cdot \sigma_Y^2 = \frac{1}{Y_0^2} \cdot \sigma_{ET}^2 + \frac{ET_0^2}{Y_0^4} \cdot \sigma_Y^2 \\ &= \frac{ET_0^2}{Y_0^2} \cdot \frac{\sigma_{ET}^2}{ET_0^2} + \frac{ET_0^2}{Y_0^2} \cdot \frac{\sigma_Y^2}{Y_0^2} = U_0^2 \cdot (CV_{ET}^2 + CV_Y^2) \end{aligned} \tag{30}$$

where the subscript 0 identifies the mean value.

Thus, being by definition:

$$CV_{uWF}^2 = \frac{\sigma_{uWF}^2}{U_0^2} \tag{31}$$

From Eq. (30), we obtain:

$$CV_{uWF}^2 = \sqrt{CV_{ET}^2 + CV_Y^2} \tag{32}$$

*Evaluation of the error of actual evapotranspiration estimates and yield.* We perform a comparative analysis between the yield  $Y_i(t)$  and the actual evapotranspiration  $ETA_i(t)$  estimated in our study at the municipality scale (in the following indicated as the generic variable  $x_i(t)$ ) with respect to reference data in the literature (indicated as  $x_{i,ref}(t)$ ) for a specific year  $t$  within the period of study (2004–2018). The squared deviation  $s_{x,i}^2$  of our estimate  $x_i$  from the reference value ( $x_{ref}$ ) at the municipality scale reads as:

$$s_{x,i}^2 = (x_i - x_{i,ref})^2 \tag{33}$$

and the standard deviation is:

$$\sigma_{x,i} = \sqrt{s^2} = \sqrt{(x_i - x_{i,ref})^2} \tag{34}$$

we obtain:

$$CV_{x,i} = \frac{\sigma}{x_{ref}} = \frac{\sqrt{(x_i - x_{i,ref})^2}}{x_{i,ref}} = \frac{|(x_i - x_{i,ref})|}{x_{i,ref}} \tag{35}$$

We then calculate the mean  $CV_x$  over traced municipalities in the reference year  $t$ , as:

$$CV_x = \frac{\sum_{i=1}^M CV_{x,i} \cdot T_i}{\sum_{i=1}^M T_i} \tag{36}$$

where  $M$  is the total number of traced municipalities and  $T_i(t)$  are the traded soy volumes for each municipality  $i$  in the year  $t$ .

The yield data provided by TRASE ( $Y_i$ ) are compared with the values provided by the SPAM2010 dataset<sup>69</sup> ( $Y_{i,ref}$ ), while actual evapotranspiration estimates obtained in this study ( $ET_i$ ) have been compared with the estimates provided by the WATNEEDS model<sup>71</sup> ( $ET_{i,ref}$ ). To perform the analyses, gridded values at the pixel level both by SPAM2010 and WATNEEDS are averaged at the scale of municipality  $i$ .

Since SPAM2010 is centred in 2010, we compare the SPAM yields with our estimation  $Y_i(2010)$  for 2010. The WATNEEDS model provides estimates for soy evapotranspiration for the years 2000 and 2016, thus we perform the error analysis with respect to the year 2016, referring to  $ET_i(2016)$ , which is the year that intersects our period of study 2004–2018. For the year 2016, we weigh the irrigated and rainfed components of the evaporation estimates of green and blue water—both for our and the WATNEEDS model—with the rainfed and irrigated areas provided by SPAM2010<sup>69</sup> as in Eqs. (14) and (15).

We find good agreement between our estimates and reference data for yield obtaining a  $CV_Y$  equal to 8%, while we find a  $CV_{ET}$  equal to 15% for soy evapotranspiration estimates. The cumulated relative frequency curves (Supplementary Fig. 8) show that, over the traced municipalities, we obtain for the 50% of them a  $CV_{Y,i}$  less than 5% referring to the year 2010 and a  $CV_{ET,i}$  less than 15% referring to the year 2016.

Finally, considering Eq. (32), a  $CV_{uWF}$  equal to 17% is obtained for the uWF.

**Table 1 Uncertainty of: yield ( $CV_Y$ ), evapotranspiration ( $CV_{ET}$ ), unit water footprint ( $CV_{uWF}$ ), traded tons ( $CV_T$ ), and traded virtual water volume ( $CV_{VWT}$ ) estimates.**

$CV_Y$	$CV_{ET}$	$CV_{uWF}$	$CV_T$	$CV_{VWT}$
8%	15%	17%	5%	18%

*Propagation of the uncertainty to the VWT.* We propagate the uncertainty to the VWT (Eq. (19)) according to:

$$\sigma_{VWT}^2 = uWF_0^2 \cdot \sigma_T^2 + T^2 \cdot \sigma_{uWF}^2 = uWF_0^2 \cdot T_0^2 \cdot CV_T^2 + T_0^2 \cdot uWF_0^2 \cdot CV_{uWF}^2 \tag{37}$$

which becomes:

$$CV_{VWT}^2 = CV_T^2 + CV_{uWF}^2 \tag{38}$$

where  $CV_T$  is calculated with Eq. (4) and  $CV_{uWF}$  with Eq. (32).

We finally find a  $CV_{VWT}$  of 18%.

We summarize in Table 1 the uncertainty of each component of the VWT analysis. We find that overall the differences obtained, given the context, the type of data, and the complex nature of the variables involved (especially for the estimate of the actual evapotranspiration) are to be considered small. Therefore, the error and comparative analyses performed give strength to what is presented and discussed in the paper.

We contacted the nine TNCs considered in this study (ADM, Amaggi, Bianchini S.A, Bunge, Cargill, COFCO, Gavilon, Glencore and Louis Dreyfus) for comment about our findings. We received a response from Cargill, who have pointed us to their ESG report<sup>72</sup> acknowledging their role in water stewardship.

### Data availability

All the input data used in this study are from publicly available sources. Country data on bilateral trade matrices are available from the FAOSTAT Data Statistics (<http://www.fao.org/faostat/en/#data>). Site- and company-specific trade data are available from the TRASE dataset (<https://www.trase.earth/>). The global self-calibrated Palmer Index (1901–2021 using preliminary CRU TS 4.06, 0.5° lat-lon resolution) is available at <https://crudata.uea.ac.uk/cru/data/drought/>. The dataset generated in the current study is available at <https://doi.org/10.5281/zenodo.7334623>.

### Code availability

The codes developed for the analyses and to generate results are available from the corresponding author on reasonable request.

Received: 26 June 2022; Accepted: 3 March 2023;

Published online: 22 March 2023

### References

- Dalin, C., Wada, Y., Kastner, T. & Puma, M. J. Groundwater depletion embedded in international food trade. *Nature* **543**, 700–704 (2017).
- D’Odorico, P. et al. Global virtual water trade and the hydrological cycle: patterns, drivers, and socio-environmental impacts. *Environ. Res. Lett.* **14**, 053001 (2019).
- Soligno, I., Ridolfi, L. & Laio, F. The environmental cost of a reference withdrawal from surface waters: definition and geography. *Adv. Water Resour.* **110**, 228–237 (2017).
- Rosa, L., Chiarelli, D. D., Tu, C., Rulli, M. C. & D’Odorico, P. Global unsustainable virtual water flows in agricultural trade. *Environ. Res. Lett.* **14**, 114001 (2019).
- Wang-Erlandsson, L. et al. A planetary boundary for green water. *Nat. Rev. Earth Environ.* **3**, 380–392 (2022).
- Vanham, D. et al. Environmental footprint family to address local to planetary sustainability and deliver on the SDGs. *Sci. Total Environ.* **693**, 133642 (2019).
- Wiedmann, T. & Lenzen, M. Environmental and social footprints of international trade. *Nat. Geosci.* **11**, 314–321 (2018).
- D’Odorico, P., Carr, J. A., Laio, F., Ridolfi, L. & Vandoni, S. Feeding humanity through global food trade. *Earths Future* **2**, 458–469 (2014).
- Allan, J. A. Virtual water—the water, food, and trade nexus. Useful concept or misleading metaphor? *Water Int.* **28**, 106–113 (2003).
- Komar, M. et al. Water for food: the global virtual water trade network. *Water Resour. Res.* <https://doi.org/10.1029/2010WR010307> (2011).

11. Aldaya, M. M., Chapagain, A. K., Hoekstra, A. Y. & Mekonnen, M. M. *The Water Footprint Assessment Manual: Setting the Global Standard* (Routledge, 2012).
12. Dalin, C., Konar, M., Hanasaki, N., Rinaldo, A. & Rodriguez-Iturbe, I. Evolution of the global virtual water trade network. *Proc. Natl Acad. Sci. USA* **109**, 5989–5994 (2012).
13. D’Odorico, P. et al. The global food-energy-water nexus. *Rev. Geophys.* **56**, 456–531 (2018).
14. Tamea, S., Tuninetti, M., Soligno, I. & Laio, F. Virtual water trade and water footprint of agricultural goods: the 1961–2016 CWASI database. *Earth Syst. Sci. Data* **13**, 2025–2051 (2020).
15. Dalin, C., Hanasaki, N., Qiu, H., Mauzerall, D. L. & Rodriguez-Iturbe, I. Water resources transfers through Chinese interprovincial and foreign food trade. *Proc. Natl Acad. Sci. USA* **111**, 9774–9779 (2014).
16. Harris, F. et al. Trading water: virtual water flows through interstate cereal trade in India. *Environ. Res. Lett.* **15**, 125005 (2020).
17. Karakoc, D. B., Wang, J. & Konar, M. Food flows between counties in the United States from 2007 to 2017. *Environ. Res. Lett.* **17**, 034035 (2022).
18. Flach, R., Ran, Y., Godar, J., Karlberg, L. & Suavet, C. Towards more spatially explicit assessments of virtual water flows: linking local water use and scarcity to global demand of Brazilian farming commodities. *Environ. Res. Lett.* **11**, 075003 (2016).
19. Folke, C. et al. Transnational corporations and the challenge of biosphere stewardship. *Nat. Ecol. Evol.* **3**, 1396–1403 (2019).
20. Rockström, J. et al. We need biosphere stewardship that protects carbon sinks and builds resilience. *Proc. Natl Acad. Sci. USA* **118**, e2115218118 (2021).
21. Rudebeck, T. in *Corporations as Custodians of the Public Good?* 1–17 (Springer, 2019).
22. Österblom, H. et al. Transnational corporations as ‘keystone actors’ in marine ecosystems. *PLoS ONE* **10**, e0127533 (2015).
23. Folke, C. et al. An invitation for more research on transnational corporations and the biosphere. *Nat. Ecol. Evol.* **4**, 494 (2020).
24. Virdin, J. et al. The ocean 100: transnational corporations in the ocean economy. *Sci. Adv.* **7**, eabc8041 (2021).
25. Folke, C. & Kautsky, N. Aquaculture and ocean stewardship. *Ambio* **51**, 13–16 (2022).
26. Godar, J. Supply chain mapping in trase. Summary of data and methods. [http://resources.trase.earth/documents/Trase\\_supply\\_chain\\_mapping\\_manual.pdf](http://resources.trase.earth/documents/Trase_supply_chain_mapping_manual.pdf) (2018).
27. Trase. Trase earth data tools. <https://trase.earth/explore> (2023).
28. Croft, S. A., West, C. D. & Green, J. M. Capturing the heterogeneity of sub-national production in global trade flows. *J. Cleaner Prod.* **203**, 1106–1118 (2018).
29. IBGE. Instituto brasileiro de geografia e estatística. <https://www.ibge.gov.br/> (2023).
30. Souza, C. M. et al. Reconstructing three decades of land use and land cover changes in Brazilian biomes with landsat archive and earth engine. *Remote Sens.* **12**, 2735 (2020).
31. Colli, G. R., Vieira, C. R. & Dianese, J. C. Biodiversity and conservation of the cerrado: recent advances and old challenges. *Biodivers. Conserv.* **29**, 1465–1475 (2020).
32. Van der Ent, R. J., Savenije, H. H., Schaeffli, B. & Steele-Dunne, S. C. Origin and fate of atmospheric moisture over continents. *Water Resour. Res.* <https://doi.org/10.1029/2010WR009127> (2010).
33. Peña-Arancibia, J. L., Bruijnzeel, L. A., Mulligan, M. & Van Dijk, A. I. Forests as ‘ponges’ and ‘pumps’: assessing the impact of deforestation on dry-season flows across the tropics. *J. Hydrol.* **574**, 946–963 (2019).
34. FAOSTAT. Crop production. <http://www.fao.org/faostat/en/#data/QC> (2023).
35. Trase. Who dominates the trade in Brazilian soy? <http://resources.trase.earth/documents/infobriefs/infobrief1.pdf> (2017).
36. Trase. Illegal deforestation and Brazilian soy exports: the case of Mato Grosso. <https://www.icv.org.br/website/wp-content/uploads/2020/06/traseissuebrief4-en.pdf> (2020).
37. Trase. Who is buying soy from MATOPIBA? <http://resources.trase.earth/documents/infobriefs/Infobrief2.pdf> (2018).
38. Grabs, J. & Carodenuto, S. L. Traders as sustainability governance actors in global food supply chains: a research agenda. *Business Strategy Environ.* **30**, 1314–1332 (2021).
39. Getirana, A., Libonati, R. & Cataldi, M. Brazil is in water crisis—it needs a drought plan. *Nature* **600**, 218–220 (2021).
40. Khanna, J., Medvigy, D., Fueglistaler, S. & Walko, R. Regional dry-season climate changes due to three decades of Amazonian deforestation. *Nat. Clim. Chang.* **7**, 200–204 (2017).
41. Leite-Filho, A. T., de Sousa Pontes, V. Y. & Costa, M. H. Effects of deforestation on the onset of the rainy season and the duration of dry spells in Southern Amazonia. *J. Geophys. Res. Atmos.* **124**, 5268–5281 (2019).
42. Xu, X. et al. Deforestation triggering irreversible transition in Amazon hydrological cycle. *Environ. Res. Lett.* **17**, 034037 (2022).
43. Christian, J. I. et al. Global distribution, trends, and drivers of flash drought occurrence. *Nat. Commun.* **12**, 1–11 (2021).
44. Pousa, R. et al. Climate change and intense irrigation growth in western Bahia, Brazil: the urgent need for hydroclimatic monitoring. *Water* **11**, 933 (2019).
45. Österblom, H., Bebbington, J., Blasiak, R., Sobkowiak, M. & Folke, C. Transnational corporations, biosphere stewardship, and sustainable futures. *Annu. Rev. Environ. Resour.* **47**, 609–637 (2022).
46. Leite-Filho, A. T., Soares-Filho, B. S., Davis, J. L., Abrahão, G. M. & Börner, J. Deforestation reduces rainfall and agricultural revenues in the Brazilian Amazon. *Nat. Commun.* **12**, 1–7 (2021).
47. Ren, D. et al. The land-water-food-environment nexus in the context of China’s soybean import. *Adv. Water Resour.* **151**, 103892 (2021).
48. Agência Nacional de Águas. *Atlas Irrigação: Uso da Água na Agricultura Irrigada* (Agência Nacional de Águas, 2017).
49. Godar, J., Suavet, C., Gardner, T. A., Dawkins, E. & Meyfroidt, P. Balancing detail and scale in assessing transparency to improve the governance of agricultural commodity supply chains. *Environ. Res. Lett.* **11**, 035015 (2016).
50. Gardner, T. A. et al. Transparency and sustainability in global commodity supply chains. *World Dev.* **121**, 163–177 (2019).
51. Trase. Exploring Brazilian soy supply chains for the Amsterdam declarations’ signatories. <https://globalcanopy.org/insights/publication/exploring-brazilian-soy-supply-chains-for-the-amsterdam-declarations-signatories/> (2018).
52. Mukherji, A. Climate change: put water at the heart of solutions. *Nature* **605**, 195 (2022).
53. Erçin, E., Veldkamp, T. I. & Hunink, J. Cross-border climate vulnerabilities of the European Union to drought. *Nat. Commun.* **12**, 1–10 (2021).
54. Hasegawa, T. et al. Extreme climate events increase risk of global food insecurity and adaptation needs. *Nat. Food* **2**, 587–595 (2021).
55. Escobar, N. et al. Spatially-explicit footprints of agricultural commodities: mapping carbon emissions embodied in Brazil’s soy exports. *Glob. Environ. Chang.* **62**, 102067 (2020).
56. Green, J. M. et al. Linking global drivers of agricultural trade to on-the-ground impacts on biodiversity. *Proc. Natl Acad. Sci. USA* **116**, 23202–23208 (2019).
57. Gatti, L. V. et al. Amazonia as a carbon source linked to deforestation and climate change. *Nature* **595**, 388–393 (2021).
58. Doughty, C. E. et al. Drought impact on forest carbon dynamics and fluxes in Amazonia. *Nature* **519**, 78–82 (2015).
59. Aragão, L. E. The rainforest’s water pump. *Nature* **489**, 217–218 (2012).
60. Aragão, L. E. et al. 21st century drought-related fires counteract the decline of Amazon deforestation carbon emissions. *Nat. Commun.* **9**, 1–12 (2018).
61. FAOSTAT. Detailed trade matrix. <http://www.fao.org/faostat/en/#data/TM> (2023).
62. Mekonnen, M. & Hoekstra, A. Y. The green, blue and grey water footprint of crops and derived crops products. *Hydrol. Earth Syst. Sci.* **15**, 1577–1600 (2011).
63. Godar, J., Persson, U. M., Tizado, E. J. & Meyfroidt, P. Towards more accurate and policy relevant footprint analyses: tracing fine-scale socio-environmental impacts of production to consumption. *Ecol. Econ.* **112**, 25–35 (2015).
64. Portmann, F. T., Siebert, S. & Döll, P. Mirca2000—global monthly irrigated and rainfed crop areas around the year 2000: a new high-resolution data set for agricultural and hydrological modeling. *Glob. Biogeochem. Cycles* <https://doi.org/10.1029/2008GB003435> (2010).
65. Allen, R. G., Pereira, L. S., Raes, D. & Smith, M. et al. *Crop Evapotranspiration-Guidelines for Computing Crop Water Requirements-FAO Irrigation and Drainage Paper 56* (FAO, 1998).
66. Harris, I., Osborn, T. J., Jones, P. & Lister, D. Version 4 of the cru ts monthly high-resolution gridded multivariate climate dataset. *Sci. Data* **7**, 1–18 (2020).
67. Tuninetti, M., Tamea, S., D’Odorico, P., Laio, F. & Ridolfi, L. Global sensitivity of high-resolution estimates of crop water footprint. *Water Resour. Res.* **51**, 8257–8272 (2015).
68. Mekonnen, M. M. & Hoekstra, A. Y. National water footprint accounts: the green, blue and grey water footprint of production and consumption. Volume 1: Main report. <https://www.waterfootprint.org/media/downloads/Report50-NationalWaterFootprints-Vol1.pdf> (2011).
69. Yu, Q. et al. A cultivated planet in 2010–Part 2: The global gridded agricultural-production maps. *Earth Syst. Sci. Data* **12**, 3545–3572 (2020).
70. van der Schrier, G., Barichivich, J., Briffa, K. & Jones, P. A scpsdi-based global data set of dry and wet spells for 1901–2009. *J. Geophys. Res. Atmos.* **118**, 4025–4048 (2013).
71. Chiarelli, D. D. et al. The green and blue crop water requirement watneeds model and its global gridded outputs. *Sci. Data* **7**, 1–9 (2020).
72. Cargill. ESG report 2022. <https://www.cargill.com/doc/1432218789216/2022-esg-land-and-water.pdf> (2022).

### Author contributions

E.D.P., M.T., L.R., and F.L. designed the study. E.D.P. and M.T. conducted the analyses and E.D.P. produced the figures. E.D.P., M.T., L.R., and F.L. contributed to data

interpretation. E.D.P. and M.T. wrote the first draft of the paper. E.D.P., M.T., L.R., and F.L. edited the paper.

### Competing interests

The authors declare no competing interests.

### Additional information

**Supplementary information** The online version contains supplementary material available at <https://doi.org/10.1038/s43247-023-00742-4>.

**Correspondence** and requests for materials should be addressed to Elena De Pettillo.

**Peer review information** *Communications Earth & Environment* thanks Franco Ruzzenenti, Davy Vanham and the other, anonymous, reviewer(s) for their contribution to the peer review of this work. Primary handling editors: Michael Bank, Clare Davis. Peer reviewer reports are available.

**Reprints and permission information** is available at <http://www.nature.com/reprints>

**Publisher's note** Springer Nature remains neutral with regard to jurisdictional claims in published maps and institutional affiliations.



**Open Access** This article is licensed under a Creative Commons Attribution 4.0 International License, which permits use, sharing, adaptation, distribution and reproduction in any medium or format, as long as you give appropriate credit to the original author(s) and the source, provide a link to the Creative Commons license, and indicate if changes were made. The images or other third party material in this article are included in the article's Creative Commons license, unless indicated otherwise in a credit line to the material. If material is not included in the article's Creative Commons license and your intended use is not permitted by statutory regulation or exceeds the permitted use, you will need to obtain permission directly from the copyright holder. To view a copy of this license, visit <http://creativecommons.org/licenses/by/4.0/>.

© The Author(s) 2023